Published in final edited form as:
J Immunol. 2012 May 15; 188(10): 5003–5011. doi:10.4049/jimmunol.1103430.

Reactive Oxygen Species Produced by the NOX2 Complex in Monocytes Protect Mice from Bacterial Infections1, ,2, ,3

Angela Pizzolla[*], **Malin Hultqvist**[†,‡4], **Bo Nilson**[§], **Melissa J. Grimm**[¶], **Tove Eneljung**[‖], **Ing-Marie Jonsson**[‖], **Margareta Verdrengh**[‖], **Tiina Kelkka**[*,#,**], **Inger Gjertsson**[‖], **Brahm H. Segal**[¶,††,‡‡], and **Rikard Holmdahl**[*,†,**]

[*]Medical Inflammation Research, MBB, Karolinska Institutet, Stockholm, Sweden [†]Medical Inflammation Research, BMC, Lund University, Lund, Sweden [§]Section of Medical Microbiology, Lund University, Lund, Sweden [¶]Dept. of Medicine, Roswell Park Cancer Institute, Buffalo, New York, USA [‖]Department of Rheumatology and Inflammation Research, University of Gothenburg, Gothenburg, Sweden [#]Turku Graduate School of Biomedical Sciences, Turku, Finland [**]Medical Inflammation Research, Medicity, Turku, Finland [††]Department of Immunology, Roswell Park Cancer Institute [‡‡]Department of Medicine, School of Medicine and Biomedical Sciences, University of Buffalo, Buffalo, New York, USA

Abstract

Chronic granulomatous disease (CGD) is an inherited disorder characterized by recurrent life-threatening bacterial and fungal infections. CGD results from defective production of reactive oxygen species (ROS) by phagocytes caused by mutations in genes encoding the NADPH oxidase 2 (NOX2) complex subunits. Mice with a spontaneous mutation in *Ncf1*, which encodes the NCF1 (p47^{phox}) subunit of NOX2, have defective phagocyte NOX2 activity. These mice occasionally develop local spontaneous infections by *Staphylococcus xylosus* or by the common CGD pathogen *S. aureus*. *Ncf1* mutant mice were more susceptible to systemic challenge with these bacteria than wild type mice. Transgenic *Ncf1* mutant mice harboring wild type *Ncf1* gene under the human CD68 promoter (MN+ mice) gained the expression of NCF1 and functional NOX2 activity specifically in monocyte/macrophages, although minimal NOX2 activity was detected also in some CD11b+Ly6G+ cells defined as neutrophils. MN+ mice did not develop spontaneous infection and were more resistant to administered staphylococcal infections compared to MN− mice. Most strikingly, MN+ mice survived after administered *Burkholderia cepacia*, an

[1]This work was supported by the Swedish Research Council, the Swedish Strategic Science Foundation, the Academy of Finland, the European Union grants BeTheCure and Masterswitch (HEALTH-F2-2008-223404), the NIAID R01AI079253 (BHS), NCI Cancer Center and support Grant to Roswell Park Cancer Institute (CA016056).

[3]Abbreviations:
CGD: Chronic granulomatous disease
DHR: dehydrorhodamine
NCF1: neutrophils cytosolic factor 1
NOX2: NADPH oxidase 2 complex
ROS: reactive oxygen species
DC: Dendritic cell

[2]Corresponding author: Rikard Holmdahl, Division of Medical Inflammation Research, Department of Medical Biochemistry and Biophysics, Karolinska Institutet, 171 77 Stockholm, Sweden, Rikard.Holmdahl@ki.se, Phone: +46-8-524 84607, Fax: +46-8-524-84650.
[4] [‡]Present address: Redoxis AB, Lund, Sweden

Authorships contributions
A.P. performed research, collected data, analyzed and interpreted data and wrote the manuscript. M.H. provided animals, analyzed and interpreted data. B.N., M.J.G., T.E., I-M. J., M.V. and T.K. performed research, collected data, analyzed and interpreted data. I.G., B.H.S. and R.H. designed research and wrote the manuscript.

opportunistic pathogen in CGD patients, whereas MN− mice died. Thus, monocyte/macrophage expression of functional NCF1 protected against spontaneous and administered bacterial infections.

Introduction

Chronic granulomatous disease (CGD) is an inherited disorder characterized by recurrent life-threatening bacterial and fungal infections and persistent inflammation (1). The pathogens vary according to the geographical area. In North America and Europe the majority of the infections are caused by the following pathogens: *Staphylococcus aureus, Burkholderia cepacia, Serratia marcescens, Nocardia* species, *Salmonella* species, *Aspergillus* species and other moulds (reviewed by Grimm et al. (2) and Holland (3) and (4)). The impaired host defense is due to defective production of reactive oxygen species (ROS) by phagocytes caused by mutations in genes encoding the phagocyte nicotinamide adenine dinucleotide phosphate (NADPH) oxidase 2 complex (NOX2) protein subunits (5, 6). CGD can result from recessive mutations in any of the 5 genes encoding subunits of the NOX2 complex. (4, 7). X-linked CGD results from mutations in the cytochrome b-245 heavy chain catalytic subunit (also known as gp91^{phox} or NOX2 and coded by CYBB), and accounts for approximately 70% of CGD cases, The most common form of autosomal recessive CGD results from mutations in the regulatory protein NCF1 (coded by NCF1 and also known as p47^{phox}), and accounts for 20% of CGD cases (4). Knocking out *Cybb* or *Ncf1* (the latter referred to as *Ncf1−/−*) generated mouse models of CGD that showed increased susceptibility to bacterial and fungal infections compared to wild type (wt) mice (8–11). Spontaneous bacterial and fungal infections occurred in *Ncf1−/−* mice, with soft tissue infections by *Staphylococcus xylosus* being the most common (11).

We have previously reported that a spontaneous single nucleotide mutation in the *Ncf1* gene (referred to as *Ncf1*/**) results in impaired phagocyte NADPH oxidase activity and enhanced inflammatory responses in autoimmune chronic inflammatory diseases, such as collagen induced arthritis (CIA) and experimental autoimmune encephalomyelitis (12). As human CGD is most commonly caused by single mutations, we investigated whether *Ncf1**/* mice exhibit the CGD phenotype regarding increased susceptibility to infections. We observed that *Ncf1**/* mice in separate mouse facilities occasionally developed spontaneous soft tissue infections with similar features as the ones reported in the *Ncf1−/−* mice. The most common cultured isolates were *Staphylococcus xylosus* the same strain previously isolated in *Ncf1−/−* mice (11), but also *Staphylococcus aureus*, a frequent pathogen in CGD patients. Taken together, these results show that the *Ncf1**/* mice manifest both increased susceptibility to spontaneous infections and a more severe inflammatory phenotype in experimental models of autoimmune chronic inflammation. The NOX2 complex is functional in both neutrophils and macrophages. While the critical role of neutrophil NOX2 in host defense is well established (13), the role of NOX2 in macrophages is less clear. Since in both CGD patients and mouse models, the NOX2 complex is deficient in all myeloid cells, it was not possible to delineate the specific contribution of macrophage NOX2 to host defense *in vivo*. Now, for the first time, we show that monocyte expression of functional NCF1 under the control of the human CD68 promoter protected mice from lethal infection by *S. xylosus* and *Burkholderia cepacia*. In conclusion, a natural occurring mutation in *Ncf1*, which impairs the protein function, limits the anti-bacterial defense in mice similarly to the human CGD condition. Transgenic mice where functional NCF1 is targeted to monocytes are protected from lethal bacterial infections. These findings are important in the dissection of the mechanisms of impaired host defense in CGD and for the development of targeted cures.

Material and Methods

Ethics statement

All procedures performed on mice were approved at the respective institutes and complied with federal guidelines. The experiments conducted at Roswell Park Cancer Institute followed the federal Animal Welfare Act and the NIH guide for the Care and Use of Laboratory Animals and were approved by the Institutional Animal Care and Use Committee under the number 1135M. Experiments carried out in Finland were approved by the Regional state administrative agency in Southern Finland under the number ESAVI-0000497/041003/2011. The ones performed in Sweden followed the Animal Protection Law (Djurskyddslag) and were approved by the Gothenburg committee with number 106-2009 and the Northern Stockholm committee under number N169/10.

Animals

All mice used were genetically controlled and shared the C57Black background. The C57BL/10.Q/rhd background was confirmed to be homozygous apart from the previously described (*Ncf1*^{m1J}/*Ncf1**) mutation in the *Ncf1* gene using a 10k SNP chip (12, 14). The MHC class II congenic C57BL/10.Q/rhd (B10.Q) mice express MHC class II H2-A^{q} that is encoded by a fragment from the DBA/1 strain. The *Ncf1* mutation impairs the function of NCF1 as described earlier (12). The B10.P.MBQ mice have been described previously (15): they are transgenic mice where H-2A^{q} is expressed under the hCD68 promoter. The B10.Q.Bko mice were previously called B10.Q.μMT mice: they were obtained from backcrossing the original μMT founder, kindly provided by Dr. Werner Müller (Institute of Genetics, Cologne, Germany), to B10.Q for more than 10 generations (16). TCRko animals were bought form Jackson laboratories (Tcrb^{tm1Mom}) and then backcrossed for more than 10 generations to B10.Q. The B10.Q.COMP ko mice were previously described and backcrossed to B10.Q for more than 10 generations. (17). B10.Q.MN mice were described previously (18): the MN transgene encodes the functional NCF1 under the hCD68 promoter. *Ncf1−/−* (also denoted p47$^{phox-/-}$) mice generated as previously described (11) were backcrossed to N14 in C57BL/6, and maintained at Roswell Park Cancer Institute, Buffalo, NY. Mice were housed under SPF conditions.

Bacterial isolates

Bacterial growth of isolated samples from infected animals was assessed on various media under different incubation conditions. All identified isolates could be cultured on hematin agar at 37°C under aerobic conditions. Species identification was based on 16S rDNA sequence analysis and phenotypic tests. Cultured colonies was suspended in 100 μl H_2O and heat treated for 15 minutes at 95°C. PCR for 16S analysis was performed without further extraction of DNA and amplification was carried out in a 50-μl reaction mixture containing 1× PCR buffer (Qiagen), 3 mM $MgCl_2$, 200 μM each deoxynucleoside triphosphate, 1.0 U of HotStar *Taq* DNA polymerase (Qiagen), 10 pmol of each primer, and 5 μl of DNA template. P8F (5′- AGA GTT TGA TCM TGG CTC AG-3′) (19) and P911r (5′-CCC GTC AAT TCH TTT GAG T-3′) (20) were used as PCR and sequencing primers. A pre-PCR step of 15 min at 95°C was followed by 40 cycles of 93°C for 50 s, 52°C for 50 s, and 72°C for 50 s. A final step of 5 min at 72°C terminated the amplification. Tubes with no target DNA and *Escherichia coli* DNA were included as negative and positive controls, respectively. Both strands of the approximately 800-bp PCR product were sequenced using the BigDye Terminator Cycle Sequencing kit (Applied Biosystems Inc., Foster City, CA) and analyzed on an ABI PRISM 3100 Genetic Analyzer (Applied Biosystems Inc.) by BMLabbet (Furulund, Sweden). The sequences of the isolates were identical to the 16S rRNA genes either of *Staphylococcus aureus, Staphylococcus saprophyticus/xylosus* or *Escherichia coli* available at the National Center for Biotechnology Information

(www.ncbi.nlm.nih.gov). Strains determined to belong to the family of *S. saprophyticus* and *S. xylosus* with 16S were differentiated and identified to be *S. xylosus* by their property to ferment xylose and mannose in oxidative-fermentative medium (21).

Strain typing

The *S. xylosus* isolates were typed using automated repetitive PCR (rep-PCR) (DiversiLab) as recommended by the manufacturer. DNA was extracted using the UltraClean Microbial DNA isolation kit (MO BIO Laboratories, Carlsbad, CA) and a minimum of 50 ng DNA was then amplified using the *Staphylococcus* fingerprinting kit (Diversi- Lab; bioMérieux) according to the manufacturer's instructions. PCR products were separated on DiversiLab LabChips (bioMérieux) utilizing a 2100 Bioanalyzer (Agilent Technologies, Santa Clara, CA) operating the DiversiLab v1.4 assay. Bioanalyzer data were exported to a DiversiLab website and analyzed with DiversiLab v3.4 software. Data analysis was performed with the web-based software using the Pearson coefficients to determine distance matrices and the unweighted pair group method with arithmetic mean to create dendrograms. The DiversiLab data generated for each organism included a dendrogram with virtual gel images, a graph of fluorescence intensity that corresponds to the organism's banding pattern, and a similarity matrix. Cluster analysis was done by comparing the automated rep-PCR pattern for each isolate to a representative rep-PCR pattern obtained for each of the reference strains. Strain relatedness for the replicate studies was defined as a minimum of 90% similarity with a difference of up to 3 bands.

Systemic administration of bacteria

S. xylosus strains 720 and 1056B and *S. aureus* LS-1 and 1056A were inoculated intravenously (i.v.) in the tail vein in a total volume of 200 μl phosphate-buffered saline (PBS)/mouse. Viable counts were performed to determine the number of bacteria injected. The mice received the following number of bacteria: *S. xylosus* 1056B $0.8–1.2\times10^8$ bacteria/mouse, *S. xylosus* 720 1.4×10^8 bacteria/mouse, *S. aureus* LS-1 5.7×10^7 bacteria/mouse and *S. aureus* 1056A 0.8×10^8 bacteria/mouse. We used a strain of *Burkholderia cepacia* isolated from a CGD patient, as previously described (22). Mice were administered 4.5×10^5 CFU intraperitoneal (i.p.), an inoculum previously known to be lethal in $p47^{phox-/-}$ mice, but not in wildtype mice (22).

Bacterial counts in organs

Organs were aseptically dissected, homogenized, serially diluted in PBS and spread on agar plates. In *B. cepacia* experiments, peritoneal lavage was performed with 10 ml of DPBS. The number of colony forming units (CFUs) per site was determined after 24–48 h of incubation at 37°C.

Arthritis scoring

All mice were followed up individually and checked daily. Mice were graded blindly for arthritis severity and frequency. Finger/toe and ankle/wrist joints were inspected and arthritis was defined as visible erythema and or swelling. To evaluate the intensity of arthritis, a clinical scoring (arthritic index) was carried out using a system where macroscopic inspection yielded a score of 0–3 points for each limb (0, neither swelling nor erythema; 1, mild swelling and/or erythema; 2, moderate swelling and erythema; 3, marked swelling and erythema). The total score was calculated by adding up all the scores within each animal tested.

The overall condition of each mouse was also examined daily by assessing signs of systemic inflammation, i.e., weight decrease, reduced alertness, and ruffled coat. In cases of severe

systemic infection, when a mouse was judged too ill to survive another 24 h, it was culled and defined as dead due to sepsis.

Enrichment of neutrophils from bone marrow with Percoll gradient

Bone marrow from femurs and tibiae were extracted by flushing the bones with PBS using a 26G needle. Red blood cells were lysed with ACK buffer and the cells washed with PBS before resuspending them in 3 ml 45% Percoll solution. A Percoll gradient was formed in a 15 ml tube, loading 3 ml of 66% Percoll followed by 2 ml of 60%, 2 ml of 55% and finally adding the cells. After 30 min centrifugation at 3000 rpm with brakes off, the 66-60% interface layer of cells was recovered. All solutions and operations were at room temperature. This method leads to a myeloid preparation consisting of ~ 90% neutrophils based on cytology.

Antibodies

Pacific Blue labeled anti-CD11b (Mac-1, M1/70) antibody and PE-Cy7 or PE labeled anti-Ly6G (1A8) (from BD Biosciences) and anti-FcR (24G2, generated in our laboratory) were used to stain the blood samples. Intracellular staining for Ncf1 was performed with antibody mouse anti human Ncf1 D10 (Santa Cruz) and detected with anti-mouse IgG1-APC (BD Biosciences).

Oxidative burst assay and flow cytometry

20 μl of freshly drawn blood were stained for ROS production as described previously (23). FcR interaction was blocked with anti-FcR blocker 24G2 before incubation with the surface markers antibodies, Pacific Blue anti-CD11b (Mac-1) antibody and PE-cy7 anti-Ly6G (BD Biosciences). DHR123 (Sigma) was added to the cells at a concentration of 3 nM and the cells were stimulated with phorbol 12-myristate 13-acetate (PMA) at a concentration of 200 ng/ml. After washing, 2×10^5 cells were acquired with a BD LSRII flow cytometer and the data analyzed with FlowJo version 8.8.6.

For NCF1 intracellular staining, after incubation with surface marker antibodies and washing in PBS, the cells were fixed and permeabilized with Cytofix/CytoPerm (BD Biosciences) and subsequently stained with anti-NCF1 antibody and anti-mouse IgG1-APC according to manufacturer instructions. NCF1 expression was measured as difference between the Geo mean of cells stained with anti-NCF1 antibody and the anti-mouse IgG1-APC and the geo mean of cells stained with only the anti-mouse IgG1-APC: the Δ Geo mean is represented.

In vivo ROS detection

Naïve mice were anaesthetized with isofluorane and injected i.p. with 20 mg/kg L-012 (8-amino-5-chloro-7-phenylpyrido[3,4-d]pyridazine-1,4(2H,3H)dione) probe (Wako Chemicals) dissolved in physiological saline (24). The luminescent signal was detected with IVIS 50 bioluminescent system (Xenogen), consisting of an anesthesia unit in a light tight chamber with a CCD camera IVIS 132323, DW434. Image acquisition and analysis were performed with Living Image software (Xenogen).

Histology

Infected and healthy paws were collected and fixed in 4% paraformaldehyde buffered solution. The skin was removed and the paws were decalcified in a solution of 4% paraformaldehyde and formic acid (1:1) for 48 hr. After dehydration, paws were embedded in paraffin and sectioned (10 or 4 μm) before staining with hematoxylin-eosin or Gram staining.

Statistical methods

Mann-Whitney U test was used to compare two groups. For comparison of three groups, Kruskal-Wallis with Dunn's comparison post-test was used. For incidence comparisons, Fisher's exact test was used. Survival curves were displayed by Kaplan-Meier and intergroup comparisons assessed by the log-rank method. GraphPad Prism, version 5.0c, was used for statistical analysis. $P < 0.05$ was considered statistically significant.

Results

Spontaneous inflammation in soft tissue of Ncf1 mutant mice

We observed local spontaneous infections in *Ncf1* mutant (*Ncf1*/**) but not in *Ncf1* wt mice in the our mouse colonies in two different animal facilities, one being a conventional facility in Lund and one being a SPF, Felasa II facility in Stockholm. All the mice shared the C57Bl/10.Q.rhd background and carried the *Ncf1* mutation, but their genotype varied with respect to other congenic fragments and transgenes (table I). The frequency of observed infections averaged 2% of 2600 B10.Q.*Ncf1*/** mice. Infections occurred most commonly in the paws, but were also found in the tail, limbs, head and neck soft tissue. The inflamed tissue was swollen, red and infiltrated with pus, and was generally associated with scarring (fig 1 A and B). Histology revealed massive cell infiltration in the skin and bone, sometimes associated with bone necrosis (fig 1 C–E). In the abscesses, several bacterial colonies were present (fig 1 F), where Gram positive cocci were visible (fig 1 H), together with a large number of neutrophils and macrophages (fig 1 G). Splendore-Hoeppli material was observed around necrotic leukocytes and cell debris and inside necrotic macrophages (fig 1 G). Infections were more common in males than females.

Usually, several, if not all, mice in a cage developed infection, raising the possibility of transmitted infection. Interestingly, we also observed the same infection frequency in B10.Q.*Ncf1*/** mice (but not in NOX2-competent mice) with specific engineered cell or protein deficiencies, including deficiency in B cells or T cells, deletion of cartilage oligomeric matrix protein (COMP) (17) or deficient expression of specific MHC class II alleles on macrophages (15), all on the same B10.Q genetic background.

To characterize the bacterial strains responsible for the infections, samples from infected animals were assessed. All isolates could be grown on hematin agar at 37°C under aerobic conditions. Species identification was based on 16S rDNA sequence analysis and phenotypic tests. The sequences of the isolates were identical to the 16S rRNA genes either of *Staphylococcus aureus* or *Staphylococcus saprophyticus/xylosus*. The *S. aureus* strain was denominated 1056A. Strains determined to belong to the family of *S. saprophyticus* and *S. xylosus* with 16S were differentiated and identified to be *S. xylosus* by their property to ferment xylose and mannose in oxidative-fermentative medium (21). Two *S. xylosus* strains were further characterized using the DiversiLab platform and were denominated *S. xylosus* 720 and *S. xylosus* 1056B. Interestingly all investigated samples from the animal house in Lund carried the *S. xylosus* 720 strain, whereas all samples from the Stockholm facility were either the *S. xylosus* 1056B or the *S aureus* 1056A strains. Thus, B10.Q.*Ncf1*/** mice exhibited increased susceptibility to spontaneous staphylococcal infections, with the mouse facility influencing the acquisition of specific bacterial strains.

Administered Staphylococcus xylosus and Staphylococcus aureus infections induced higher mortality in Ncf1 mutant mice compared with Ncf1 wt mice

Based on our observations of spontaneous infections in *Ncf1*/** mice, we evaluated susceptibility of *Ncf1**/* versus *Ncf1* wt (*Ncf1+/+*) mice to systemic infection. About 1×10^8 CFU of the isolated staphylococcal strains *S. xylosus* 720 and 1056B or *S. aureus* 1056A

were injected intravenously (i.v.) in *Ncf1*/** and *Ncf1+/+* mice. The *Ncf1**/* mice were more sensitive to infection than *Ncf1+/+* mice based on mortality (fig 2 B, D and F). The bacteria differed greatly in virulence: *S. xylosus* 720 and the *S. aureus* 1056A caused lethal infection while the *S. xylosus* 1056B did not result in lethality in *Ncf1*/** mice (figure 2 B, D and F).

Weight loss observed during the infection was comparable in the *Ncf1*$^{*/*}$ and *Ncf1*+/+ mice (fig 2 A, C, E). The analysis of this parameter is however heavily affected by the high mortality in the *Ncf1**/* group as only few surviving *Ncf1**/* mice could be evaluated for weight loss. These data indicate that the *Ncf1*/** mice are more susceptible to systemic *S. xylosus* (with variability in strain virulence) and *S. aureus* infection than *Ncf1* +/+ mice.

Staphylococcus aureus-induced arthritis was less severe in Ncf1 mutant as compared with Ncf1 wt mice

We have previously shown that experimental autoimmune arthritis is more severe in *Ncf1*/** compared with *Ncf1+/+* mice (12). To investigate whether this is also the case with septic arthritis we injected 5.7×10^7 *S. aureus LS-1* bacteria i.v. into *Ncf1*$^{*/*}$ and *Ncf1*+/+ mice. The *LS-1* strain of *S. aureus* was selected because of its propensity to cause septic arthritis in mice (25). Both groups developed arthritis with a similar frequency, but *Ncf1*+/+ mice had significantly greater arthritic severity (fig 3 A and B). *Ncf1*/** mice lost more weight compared to *Ncf1*+/+ littermates (fig 3 C), and had a higher bacterial count in the kidneys after bacterial injection (fig 3 D). No significant difference between the genotypes was observed in bacterial counts from blood at day 1 and 3 after infection (data not shown). Histology showed infiltration of cells into the joints and tissue and bone destruction (fig 3 E–F). These data indicate that *Ncf1*/** mice have impaired clearance of bacteria, but a milder septic arthritis than *Ncf1+/+* mice. Since *Ncf1*/** mice are prone to more severe autoimmune chronic arthritis (12), our results suggest that NOX2 has distinct roles in modulating the inflammatory response in autoimmune and septic arthritis.

Expression of Ncf1 in monocytes protects from infection after Staphylococcus aureus and Staphylococcus xylosus infection

Previously, we generated transgenic mice (transgene designated, MN) on the B10.Q.*Ncf1*/** background (*Ncf1*/* MN+/−*) that express the functional form of NCF1 through the human CD68 promoter, leading to restricted expression of NCF1 to monocytes and macrophages. *Ncf1*/* MN+/−* mice were partially protected from autoimmune arthritis compared to *Ncf1*/** mice (18). We observed that *Ncf1*/* MN+/−* mice did not develop spontaneous infections, and thus it became relevant to investigate whether *Ncf1*/* MN+/−* mice were protected from administered infections.

We previously reported that in *Ncf1*/* MN+/−* mice, NCF1 is specifically expressed on CD68 positive macrophages and not on other cells such as B cells and T cells (18), and we have now confirmed that it is not expressed in neutrophils, defined as CD11b+Ly6G+ expressing cells (26) (fig 4 A and supplementary fig 1 A and D). In *Ncf1*/* MN+/−* mice, there was full expression of NCF1 in monocyte/macrophages (CD11b+Ly6G− cells) comparable to the levels in wild type monocytes/macrophages, but no expression in neutrophils (CD11b+Ly6G+ cells), as investigated in cells from bone marrow, blood and spleen (fig 4 B and supplementary fig 1 B and E). Intracellular ROS production was measured by flow cytometry using the probe dihydrorhodamine 123 (DHR123) (27), which upon oxidation emits a fluorescent signal. Phorbol 12-myristate 13-acetate (PMA) was used as activator of the NOX2 complex. Blood monocytes (CD11b+Ly6G−) from *Ncf1*/* MN+/−* mice showed about the half of the DHR staining of monocytes from *Ncf1+/+* mice (supplementary fig 1 C). Blood neutrophils (CD11b+Ly6G+) from *Ncf1*/* MN+/−* mice

had approximately 15% of the DHR staining as neutrophils from *Ncf1+/+* mice (supplementary fig 1 C). This observation was confirmed in splenic and thioglycollate-elicited peritoneal neutrophils (supplementary fig 1 F and data not shown). The discrepancy between the lack of NCF1 expression and the detectable DHR staining in neutrophils could be explained by leakage of ROS or other DHR stained products from macrophages to neutrophils after PMA stimulation *in vitro*. To examine this hypothesis, neutrophils from bone marrow were purified with a Percoll gradient, stained for CD11b and Ly6G and analyzed via flow cytometry for their capacity to oxidize DHR. PMA-stimulated ROS production from CD11b+Ly6G+ cells from *Ncf1*/* MN+* mice was minimal (< 1% of Ncf1+/+ neutrophils) but distinguishable from ROS production in CD11b+Ly6G+ cells from *Ncf1*/** mice (fig 4 C and D). In order to confirm that the monocytes ROS production in *Ncf1*/* MN+/−* mice was detectable also *in vivo* whole body imaging of ROS production was performed using the probe L-012 (24). L-012 is a sensitive luminol derivative that detects ROS in biological samples, including NOX2 derived superoxide (28). L-012 was injected i.p. in sedated naïve mice and chemiluminescent signal was recorded over time with a CCD camera. Apart from the peritoneal area where the probe was injected, the luminescent signal was best detectable in paws where fur is absent. Therefore the signal was quantified around the front paws as represented in fig 4E *In vivo* oxidative burst was higher in paws from naïve *Ncf1+/+* and *Ncf1*/* MN+/−* mice compared to *Ncf1*/** mice. The signal from *Ncf1*/* MN+/−* mice was reduced compared to wild type, as expected since in healthy joints different ROS-producing cells other than macrophages are present (fig 4F). This observation illustrates the presence of detectable NOX2 dependent ROS even in naïve animals and the crucial role of the *Ncf1* mutation in abolishing it.

We next evaluated susceptibility to administered infection in transgenic *Ncf1*/* MN+/−* mice compared to littermates negative for the transgene (*Ncf1*/**) and wt *Ncf1*+/+ mice. Mice were injected with *S. xylosus* (1×10^8 CFU i.v), and monitored for 7-day survival. *Ncf1*/** mice died within 24 hours, whereas all *Ncf1+/+* survived. Mortality was observed in 30 % of *Ncf1*/* MN+/−* on day 6 and 7 (fig. 5A). Between the surviving groups, *Ncf1*/* MN+/−* lost more weight than *Ncf1+/+* (fig 5B). Together, these data indicate that a functional NOX2 complex expressed in monocytes protects from *S. xylosus* challenge, although the transgene may not confer full protection as compared to fully NOX2-competent *Ncf1+/+* mice.

Transgenic *Ncf1*/** MN+/− mice and littermates negative for the transgene (*Ncf1*/**) and *Ncf1*+/+ mice were next evaluated for their response to the arthritogenic *S. aureus* LS-1 strain. Weight and arthritis were monitored for 7 days following bacterial administration. *Ncf1**/* male mice lost significantly more weight than *Ncf1*+/+ and *Ncf1**/* MN+/− mice. (fig 5C). No difference in lethality between the groups was observed (data not shown). Bacterial load in the kidney at day 2, 4, and 7, in synovial fluid at day 7, and in blood at day 1 did not differ among the genotypes (data not shown). Arthritis developed in all groups but with very low scores (data not shown).

Ncf1 expression in monocytes rescued mice from lethal Burkholderia cepacia infection

Burkholderia cepacia is a Gram-negative rod that can cause severe infections in CGD patients (29, 30). Studies in isolated human neutrophils showed the key role of NOX2 in killing *B. cepacia* (31). Genetically engineered *Ncf1* knock out (*Ncf1−/−* or $p47^{phox-/-}$) mice had increased susceptibility to *B. cepacia* compared to wt mice (32). To evaluate the specific contribution of monocyte NOX2 expression in the defense against *B. cepacia* we evaluated survival and bacterial clearance in *Ncf1*/* MN+* mice as compared with the *Ncf1*/* MN−* mice. Mice were challenged i.p. with a *B. cepacia* strain isolated from a CGD patient. All *Ncf1*/** mice died within 6 days after infection, while *Ncf1*/* MN+* mice had uniform survival (Figure 6A). Engineered *Ncf1−/−* mice in the C57BL/6 lineage were tested

in parallel to determine whether knockout and spontaneous mutant mice differed in response to bacterial infection. *Ncf1−/−* mice died with a similar time course as *Ncf1*/** mice, while wt C57BL/6 mice survived. Thus, spontaneous and engineered NOX2-deficient mice were highly susceptible to *B. cepacia* whereas transgenic mice with monocyte NADPH expression were protected.

We next compared clearance of *B. cepacia* at a fixed time point after bacterial challenge in *Ncf1*/* MN−* and *Ncf1*/* MN+* mice. Mice administered the same inoculum were sacrificed at 24h, a time that precedes the onset of clinical morbidity. Higher numbers of live bacteria were recovered from the peritoneum and spleens of *Ncf1*/* MN−* mice compared to *Ncf1*/* MN+* (Fig. 6B). No difference between the genotypes was observed in bacterial counts in kidneys and lungs (data not shown). The majority of blood cultures showed no growth, and no significant difference was observed between genotypes (not shown). Taken together, the survival and bacterial clearance data demonstrate protection associated with monocyte NOX2 expression against *B. cepacia*. We conclude that NCF1 expression in monocytes plays an essential role in the systemic response to both spontaneous and induced bacterial infections.

Discussion

Our results show that monocyte-specific expression of the NOX2 regulatory component, NCF1, protected mice from lethal infections with *staphylococci* and *Burkholderia cepacia*, pathogens that commonly affect CGD patients. Interestingly, a similar phenomenon has been recently described in humans regarding susceptibility to tuberculosis. A macrophage specific impairment of the core subunit of the NOX2 complex, gp91^{phox} resulted in susceptibility to tuberculous mycobacterial disease (33). These observations suggest that a functional NOX2 complex in monocytes is important for clearance of specific intra- and extracellular bacteria.

Transgenic mice in which a gene of interest is expressed under the control of the human CD68 promoter has been widely used to achieve monocyte/macrophage-restricted expression (34, 35) based on the monocyte predominance of CD68 expression. Using the same promoter we could confirm a monocyte/macrophage specific NCF1 expression in *Ncf1*/*MN+/−* versus *Ncf1**/*. A previous publication from our group shows that in *Ncf1*/*MN+/−* mice the expression of Ncf1 was undetectable in dendritic cells (DCs) (18). A more sensitive analysis revealed expression of functional NCF1 protein in DCs from *Ncf1*/*MN+/−* transgenic mice (Pizzolla A. and Holmdahl R., unpublished results). Since myeloid DCs and monocytes have a shared lineage, it is not unexpected that CD68 promoter activity would be present in both cells, as reported recently (36). NOX2 is expressed in DCs and could have a role in antigen display and priming T cell responses (37). However, the role of DCs in controlling acute bacterial infection, if any, is unclear. *Ncf1*/*MN+/−* mice showed a low but significant DHR staining indicating presence of ROS in neutrophils after activation *in vitro*. Here neutrophils are defined as CD11b+Ly6G+ cells. Even though it is difficult to formally exclude any NCF1 expression in neutrophils, we could not detect the protein by flow cytometry in blood CD11b+Ly6G+ cells. It is possible that a fraction of those cells transcribes the human CD68 promoter or that NCF1 is expressed *in vivo* due to promoter-independent expression. Kuhns et al. (38) recently showed that among CGD patients, even very low levels of neutrophil NOX2 was associated with better outcomes compared to patients with complete NOX2 deficiency. Studies of isolated neutrophils have shown that hydrogen peroxide generated by NOX2-competent cells can diffuse into intracellular compartment of bystander NOX2-deficient neutrophils (39, 40). These observations indicate how the function of ROS may not be restricted to the cell that produces it, raising the possibility that also *in vivo*, in our transgenic mice, ROS produced

by monocytes could penetrate into low bursting neutrophils, increasing their antimicrobial activity.

The importance of neutrophil ROS production in antimicrobial defense is well established (13). The critical amount of ROS-producing neutrophils necessary to protect the host is however, difficult to determine. Studies on CGD carriers and genetically corrected CGD mouse models showed that a small fraction of ROS-producing neutrophils, about 10% of the total, could efficiently protect from bacterial and fungal infection (41, 42). Nevertheless, in these studies, all phagocytes, both neutrophils and monocytes, expressed the functional NOX2 complex, and, most commonly, only the neutrophils ROS production was determined. Therefore the immunological relevance of neutrophils and monocytes separately could not be assessed.

The NOX2 complex accounts for most of the ROS production that is essential for anti-microbial defense, since mutations in any of the genes coding for the subunits of the complex leads to a CGD phenotype in humans (4, 7). The NOX2 complex also generates the majority of the ROS observed *in vivo* since the mutation in *Ncf1* abolishes the visible ROS production in both naïve (fig 4 E and F) and arthritic mice (24, 43). In addition, ROS produced by other sources such as the mitochondrial respiratory chain, have been described to have bactericidal activity in macrophage cell lines (44).

Similar to the situation in CGD patients, in mice a naturally occurring mutation in *Ncf1* increases the risk of uncontrolled bacterial infections. The infections observed in *Ncf1* mutant mice were caused by *S. aureus* and *S. xylosus. S. aureus* is a common pathogen in CGD patients (3) and is commonly found on the skin of healthy individuals, but never so far reported in mouse models of CGD. *S. xylosus* was found to cause abscesses in soft tissue of *Ncf1−/−* mice with similar characteristics to the abscesses observed in *Ncf1*/** mice (8). Environmental factors could be relevant in determining the type and frequency of infections. The conditions under which the mice were maintained and the bacterial flora carried by the handlers could explain the difference in infectious strains observed in various colonies of *Ncf1*/** and *Ncf1−/−* mice. Staphylococci are normally non-pathogenic bacteria for mice, since wt mice have not developed any infection. The infection rapidly spreads in the cage between homozygous *Ncf1*/** offspring of *Ncf1*/** parents. Males are affected more often than females. This could be due to the fact that males fight more than females resulting in wounds. A wound was always observed in the infected area and it is likely to be the access for bacteria into the soft tissue. Recently it was reported that NOX2 deficient mice develop spontaneous inflammation in their paws (45), which phenotypically resembled the infections observed in *Ncf1−/−* (11) and *Ncf1*/** animals (fig. 1A).

The involvement of cells other than phagocytes in the NOX2-dependent clearance of pathogens does not seem to play a role in spontaneous infections. The absence of B cells or T cells did not dramatically alter the frequency of spontaneous infection by staphylococci. In both mice and humans it is known that an effective immunological memory is not built after *S. aureus* infections (mechanisms reviewed by Foster (46). In addition to antimicrobial host defense, NOX2 is also a critical modulator of inflammation. Indeed, one of the characteristics of CGD is excessive inflammation, including inflammatory bowel disease, granulomatous cystitis, and pneumonitis. Macrophage NOX2 may be important in controlling inflammation. We have previously shown that monocytes/macrophage expression of NCF1 protects against autoimmune chronic inflammatory disease (18). There are a number of mechanisms by which macrophage NOX2 may limit inflammation, including internalization of apoptotic neutrophils (47–49), modulation of transcriptional factors, such as NF-κB and Nrf2 (50), modifying antigen-processing (43, 51) or regulating T cells during antigen presentation (52) and reviewed by Sareila et al. (43). A longstanding

question has been whether this is secondary to the deficient protection against infections or whether lack of oxidative burst in fact promotes inflammatory disorders. In mice, arthritis directly caused by *S. aureus* infection is in fact decreased in the ROS-deficient mice in contrast to autoimmune arthritis where we previously found that inflammation was increased (12).

In conclusion, monocyte NOX2 expression is associated with protection from spontaneous and induced bacterial infections. Further characterization of cell specific molecular mechanisms of bacterial clearance is important for elucidating the pathways involved in microbial defense and for the development of targeted cures for CGD.

Supplementary Material

Refer to Web version on PubMed Central for supplementary material.

Acknowledgments

The authors would like to thank Emma Mondoc and Dr. Ricardo Feinstein at SVA, Uppsala, for histology, Carlos and Kristina Palestro and Tomasz Klaczkowski for care of the animals.

References

1. Bridges RA, Berendes H, Good RA. A fatal granulomatous disease of childhood; the clinical, pathological, and laboratory features of a new syndrome. AMA J Dis Child. 1959; 97:387–408. [PubMed: 13636694]
2. Grimm MJ, Vethanayagam RR, Almyroudis NG, Lewandowski D, Rall N, Blackwell TS, Segal BH. Role of NADPH oxidase in host defense against aspergillosis. Med Mycol. 2011; 49(Suppl 1):S144–S149. [PubMed: 20560866]
3. Holland MS. Chronic granulomatous disease. Clin Rev Allergy Immunol. 2010; 38:3–10. [PubMed: 19504359]
4. van den Berg JM, van Koppen E, Ahlin A, Belohradsky BH, Bernatowska E, Corbeel L, Espanol T, Fischer A, Kurenko-Deptuch M, Mouy R, Petropoulou T, Roesler J, Seger R, Stasia MJ, Valerius NH, Weening RS, Wolach B, Roos D, Kuijpers TW. Chronic granulomatous disease: the European experience. PLoS One. 2009; 4:e5234. [PubMed: 19381301]
5. Segal AW, Jones OT, Webster D, Allison AC. Absence of a newly described cytochrome b from neutrophils of patients with chronic granulomatous disease. Lancet. 1978; 2:446–449. [PubMed: 79807]
6. Segal BH, Leto TL, Gallin JI, Malech HL, Holland SM. Genetic, biochemical, and clinical features of chronic granulomatous disease. Medicine (Baltimore). 2000; 79:170–200. [PubMed: 10844936]
7. Matute JD, Arias AA, Wright NA, Wrobel I, Waterhouse CC, Li XJ, Marchal CC, Stull ND, Lewis DB, Steele M, Kellner JD, Yu W, Meroueh SO, Nauseef WM, Dinauer MC. A new genetic subgroup of chronic granulomatous disease with autosomal recessive mutations in p40 phox and selective defects in neutrophil NADPH oxidase activity. Blood. 2009; 114:3309–3315. [PubMed: 19692703]
8. Pollock JD, Williams DA, Gifford MA, Li LL, Du X, Fisherman J, Orkin SH, Doerschuk CM, Dinauer MC. Mouse model of X-linked chronic granulomatous disease, an inherited defect in phagocyte superoxide production. Nat Genet. 1995; 9:202–209. [PubMed: 7719350]
9. Ju JY, Polhamus C, Marr KA, Holland SM, Bennett JE. Efficacies of fluconazole, caspofungin, and amphotericin B in Candida glabrata-infected p47phox−/− knockout mice. Antimicrob Agents Chemother. 2002; 46:1240–1245. [PubMed: 11959551]
10. Mardiney M 3rd, Jackson SH, Spratt SK, Li F, Holland SM, Malech HL. Enhanced host defense after gene transfer in the murine p47phox-deficient model of chronic granulomatous disease. Blood. 1997; 89:2268–2275. [PubMed: 9116268]
11. Jackson SH, Gallin JI, Holland SM. The p47phox mouse knock-out model of chronic granulomatous disease. J Exp Med. 1995; 182:751–758. [PubMed: 7650482]

12. Hultqvist M, Olofsson P, Holmberg J, Bäckström BT, Tordsson J, Holmdahl R. Enhanced autoimmunity, arthritis, and encephalomyelitis in mice with a reduced oxidative burst due to a mutation in the Ncf1 gene. Proc Natl Acad Sci U S A. 2004; 101:12646–12651. [PubMed: 15310853]
13. Quie PG, White JG, Holmes B, Good RA. In vitro bactericidal capacity of human polymorphonuclear leukocytes: diminished activity in chronic granulomatous disease of childhood. J Clin Invest. 1967; 46:668–679. [PubMed: 6021213]
14. Huang CK, Zhan L, Hannigan MO, Ai Y, Leto TL. P47(phox)-deficient NADPH oxidase defect in neutrophils of diabetic mouse strains, C57BL/6J-m db/db and db/+ J Leukoc Biol. 2000; 67:210–215. [PubMed: 10670582]
15. Pizzolla A, Gelderman KA, Hultqvist M, Vestberg M, Gustafsson K, Mattsson R, Holmdahl R. CD68-expressing cells can prime T cells and initiate autoimmune arthritis in the absence of reactive oxygen species. Eur J Immunol. 2011; 41:403–412. [PubMed: 21268010]
16. Svensson L, Jirholt J, Holmdahl R, Jansson L. B cell-deficient mice do not develop type II collagen-induced arthritis (CIA). Clin Exp Immunol. 1998; 111:521–526. [PubMed: 9528892]
17. Geng H, Carlsen S, Nandakumar KS, Holmdahl R, Aspberg A, Oldberg A, Mattsson R. Cartilage oligomeric matrix protein deficiency promotes early onset and the chronic development of collagen-induced arthritis. Arthritis Res Ther. 2008; 10:R134. [PubMed: 19014566]
18. Gelderman KA, Hultqvist M, Pizzolla A, Zhao M, Nandakumar KS, Mattsson R, Holmdahl R. Macrophages suppress T cell responses and arthritis development by producing Reactive Oxygen Species. J Clin Invest. 2007; 117:3020–3028. [PubMed: 17909630]
19. Goldenberger D, Schmidheini T, Altwegg M. Detection of Bartonella henselae and Bartonella quintana by a simple and rapid procedure using broad-range PCR amplification and direct single-strand sequencing of part of the 16S rRNA gene. Clin Microbiol Infect. 1997; 3:240–245. [PubMed: 11864111]
20. Fredricks ND, Relman DA. Improved amplification of microbial DNA from blood cultures by removal of the PCR inhibitor sodium polyanetholesulfonate. J Clin Microbiol. 1998; 36:2810–2816. [PubMed: 9738025]
21. Bannerman, TL. Staphylococcus, Micrococcus, and other catalase-positive cocci that grow aerobically. In: Murray, EJOBPR.; Jorgensen, JH.; Pfaller, MA.; Yolken, RH., editors. Manual of clinical microbiology. 8th ed.. Washington DC: ASM Press; 2003. p. 719-728.
22. Segal BH, Ding L, Holland SM. Phagocyte NADPH oxidase, but not inducible nitric oxide synthase, is essential for early control of Burkholderia cepacia and chromobacterium violaceum infection in mice. Infect Immun. 2003; 71:205–210. [PubMed: 12496167]
23. Hultqvist M, Olofsson P, Gelderman KA, Holmberg J, Holmdahl R. A new arthritis therapy with oxidative burst inducers. PLoS Med. 2006; 3:e348. [PubMed: 16968121]
24. Kielland A, Blom T, Nandakumar KS, Holmdahl R, Blomhoff R, Carlsen H. In vivo imaging of reactive oxygen and nitrogen species in inflammation using the luminescent probe L-012. Free Radic Biol Med. 2009; 47:760–766. [PubMed: 19539751]
25. Bremell T, Abdelnour A, Tarkowski A. Histopathological and serological progression of experimental Staphylococcus aureus arthritis. Infect Immun. 1992; 60:2976–2985. [PubMed: 1612762]
26. Daley JM, Thomay AA, Connolly MD, Reichner JS, Albina JE. Use of Ly6G-specific monoclonal antibody to deplete neutrophils in mice. J Leukoc Biol. 2008; 83:64–70. [PubMed: 17884993]
27. Rothe G, Oser A, Valet G. Dihydrorhodamine 123: a new flow cytometric indicator for respiratory burst activity in neutrophil granulocytes. Naturwissenschaften. 1988; 75:354–355. [PubMed: 3211206]
28. Daiber A, August M, Baldus S, Wendt M, Oelze M, Sydow K, Kleschyov AL, Munzel T. Measurement of NAD(P)H oxidase-derived superoxide with the luminol analogue L-012. Free Radic Biol Med. 2004; 36:101–111. [PubMed: 14732294]
29. Winkelstein JA, Marino MC, Johnston RB Jr, Boyle J, Curnutte J, Gallin JI, Malech HL, Holland SM, Ochs H, Quie P, Buckley RH, Foster CB, Chanock SJ, Dickler H. Chronic granulomatous disease. Report on a national registry of 368 patients. Medicine (Baltimore). 2000; 79:155–169. [PubMed: 10844935]

30. Sieber OF Jr, Fulginiti VA. Pseudomonas cepacia pneumonia in a child with chronic granulomatous disease and selective IgA deficiency. Acta Paediatr Scand. 1976; 65:519–520. [PubMed: 937004]

31. Speert DP, Bond M, Woodman RC, Curnutte JT. Infection with Pseudomonas cepacia in chronic granulomatous disease: role of nonoxidative killing by neutrophils in host defense. J Infect Dis. 1994; 170:1524–1531. [PubMed: 7527826]

32. Segal BH, Sakamoto N, Patel M, Maemura K, Klein AS, Holland SM, Bulkley GB. Xanthine oxidase contributes to host defense against Burkholderia cepacia in the p47(phox−/−) mouse model of chronic granulomatous disease. Infect Immun. 2000; 68:2374–2378. [PubMed: 10722648]

33. Bustamante J, Arias AA, Vogt G, Picard C, Galicia LB, Prando C, Grant AV, Marchal CC, Hubeau M, Chapgier A, de Beaucoudrey L, Puel A, Feinberg J, Valinetz E, Janniere L, Besse C, Boland A, Brisseau JM, Blanche S, Lortholary O, Fieschi C, Emile JF, Boisson-Dupuis S, Al-Muhsen S, Woda B, Newburger PE, Condino-Neto A, Dinauer MC, Abel L, Casanova JL. Germline CYBB mutations that selectively affect macrophages in kindreds with X-linked predisposition to tuberculous mycobacterial disease. Nat Immunol. 2011; 12:213–221. [PubMed: 21278736]

34. Gough PJ, Gordon S, Greaves DR. The use of human CD68 transcriptional regulatory sequences to direct high-level expression of class A scavenger receptor in macrophages in vitro and in vivo. Immunology. 2001; 103:351–361. [PubMed: 11454064]

35. Lang R, Rutschman RL, Greaves DR, Murray PJ. Autocrine deactivation of macrophages in transgenic mice constitutively overexpressing IL-10 under control of the human CD68 promoter. J Immunol. 2002; 168:3402–3411. [PubMed: 11907098]

36. Lykens JE, Terrell CE, Zoller EE, Divanovic S, Trompette A, Karp CL, Aliberti J, Flick MJ, Jordan MB. Mice with a selective impairment of IFN-gamma signaling in macrophage lineage cells demonstrate the critical role of IFN-gamma-activated macrophages for the control of protozoan parasitic infections in vivo. J Immunol. 184:877–885. [PubMed: 20018611]

37. Savina A, Jancic C, Hugues S, Guermonprez P, Vargas P, Moura IC, Lennon-Dumenil AM, Seabra MC, Raposo G, Amigorena S. NOX2 controls phagosomal pH to regulate antigen processing during crosspresentation by dendritic cells. Cell. 2006; 126:205–218. [PubMed: 16839887]

38. Kuhns DB, Alvord WG, Heller T, Feld JJ, Pike KM, Marciano BE, Uzel G, DeRavin SS, Priel DA, Soule BP, Zarember KA, Malech HL, Holland SM, Gallin JI. Residual NADPH oxidase and survival in chronic granulomatous disease. N Engl J Med. 2010; 363:2600–2610. [PubMed: 21190454]

39. Ohno Y, Gallin JI. Diffusion of extracellular hydrogen peroxide into intracellular compartments of human neutrophils. Studies utilizing the inactivation of myeloperoxidase by hydrogen peroxide and azide. J Biol Chem. 1985; 260:8438–8446. [PubMed: 2989289]

40. Rex JH, Bennett JE, Gallin JI, Malech HL, Melnick DA. Normal and deficient neutrophils can cooperate to damage Aspergillus fumigatus hyphae. J Infect Dis. 1990; 162:523–528. [PubMed: 2165113]

41. Roos D, de Boer M, Kuribayashi F, Meischl C, Weening RS, Segal AW, Ahlin A, Nemet K, Hossle JP, Bernatowska-Matuszkiewicz E, Middleton-Price H. Mutations in the X-linked and autosomal recessive forms of chronic granulomatous disease. Blood. 1996; 87:1663–1681. [PubMed: 8634410]

42. Bjorgvinsdottir H, Ding C, Pech N, Gifford MA, Li LL, Dinauer MC. Retroviral-mediated gene transfer of gp91phox into bone marrow cells rescues defect in host defense against Aspergillus fumigatus in murine X-linked chronic granulomatous disease. Blood. 1997; 89:41–48. [PubMed: 8978275]

43. Sareila O, Kelkka T, Pizzolla A, Hultqvist M, Holmdahl R. NOX2 Complex-derived ROS as Immune Regulators. Antioxid Redox Signal. 2011

44. West AP, Brodsky IE, Rahner C, Woo DK, Erdjument-Bromage H, Tempst P, Walsh MC, Choi Y, Shadel GS, Ghosh S. TLR signalling augments macrophage bactericidal activity through mitochondrial ROS. Nature. 2011; 472:476–480. [PubMed: 21525932]

45. Lee K, Won HY, Bae MA, Hong JH, Hwang ES. Spontaneous and aging-dependent development of arthritis in NADPH oxidase 2 deficiency through altered differentiation of CD11b+ and Th/Treg cells. Proc Natl Acad Sci U S A. 2011; 108:9548–9553. [PubMed: 21593419]

46. Foster TJ. Immune evasion by staphylococci. Nat Rev Microbiol. 2005; 3:948–958. [PubMed: 16322743]

47. Sanmun D, Witasp E, Jitkaew S, Tyurina YY, Kagan VE, Ahlin A, Palmblad J, Fadeel B. Involvement of a functional NADPH oxidase in neutrophils and macrophages during programmed cell clearance: implications for chronic granulomatous disease. Am J Physiol Cell Physiol. 2009; 297:C621–C631. [PubMed: 19570889]

48. Hampton MB, Vissers MC, Keenan JI, Winterbourn CC. Oxidant-mediated phosphatidylserine exposure and macrophage uptake of activated neutrophils: possible impairment in chronic granulomatous disease. J Leukoc Biol. 2002; 71:775–781. [PubMed: 11994501]

49. Fernandez-Boyanapalli RF, Frasch SC, McPhillips K, Vandivier RW, Harry BL, Riches DW, Henson PM, Bratton DL. Impaired apoptotic cell clearance in CGD due to altered macrophage programming is reversed by phosphatidylserine-dependent production of IL-4. Blood. 2009; 113:2047–2055. [PubMed: 18952895]

50. Segal BH, Han W, Bushey JJ, Joo M, Bhatti Z, Feminella J, Dennis CG, Vethanayagam RR, Yull FE, Capitano M, Wallace PK, Minderman H, Christman JW, Sporn MB, Chan J, Vinh DC, Holland SM, Romani LR, Gaffen SL, Freeman ML, Blackwell TS. NADPH oxidase limits innate immune responses in the lungs in mice. PLoS One. 5:e9631. [PubMed: 20300512]

51. Mantegazza AR, Savina A, Vermeulen M, Perez L, Geffner J, Hermine O, Rosenzweig SD, Faure F, Amigorena S. NADPH oxidase controls phagosomal pH and antigen cross-presentation in human dendritic cells. Blood. 2008; 112:4712–4722. [PubMed: 18682599]

52. Romani L, Fallarino F, De Luca A, Montagnoli C, D'Angelo C, Zelante T, Vacca C, Bistoni F, Fioretti MC, Grohmann U, Segal BH, Puccetti P. Defective tryptophan catabolism underlies inflammation in mouse chronic granulomatous disease. Nature. 2008; 451:211–215. [PubMed: 18185592]

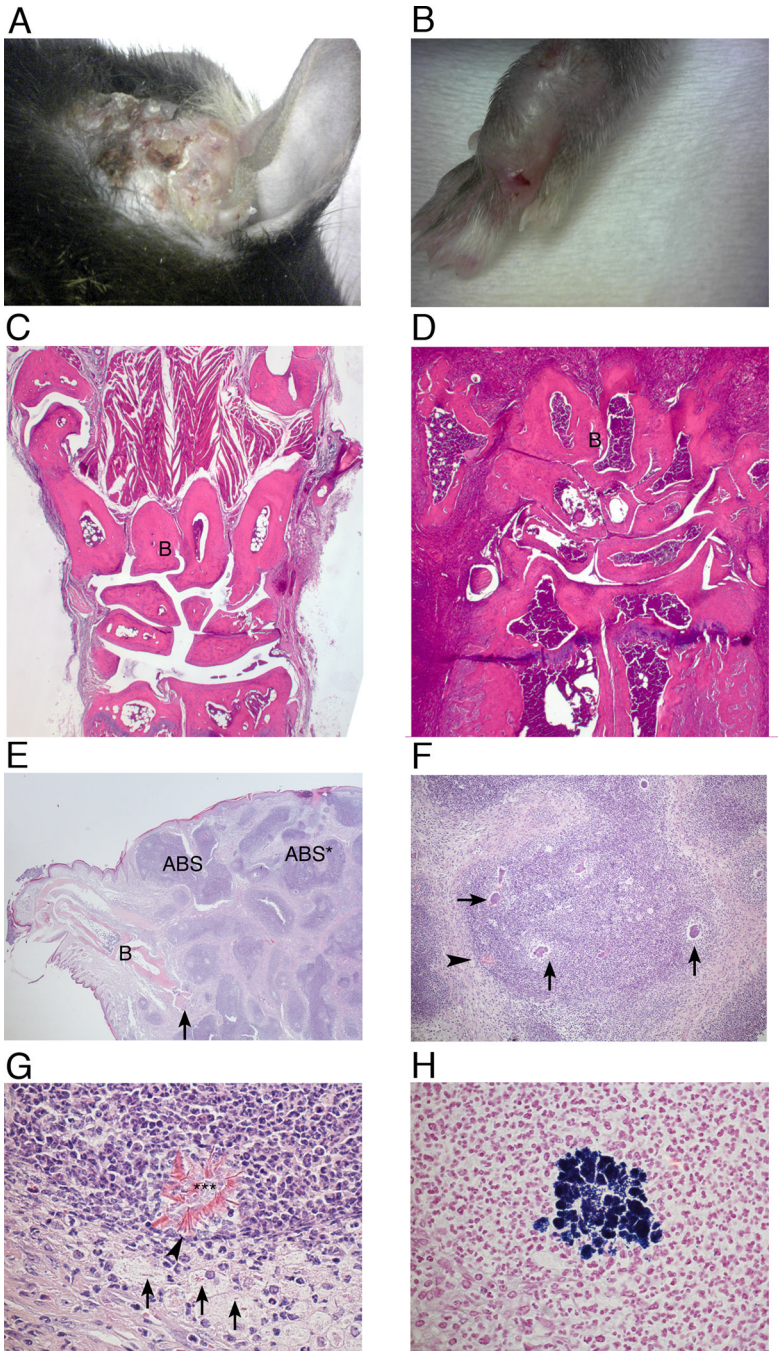

Figure 1. Spontaneous infections in soft tissue of *Ncf1* mutant mice

(A and B) Photograph of inflamed ear and paw of *Ncf1* mutant mice with spontaneous infection. (C–H) Histology of inflamed and healthy front paws. After fixation in paraformaldehyde and decalcification, the paws were sectioned and stained with hematoxylin and eosin. Front paw from a healthy mouse (C) and from an infected one (D), 2.5X magnification. (E) Markedly enlarged, inflamed paw from an infected mouse shows profound, chronic inflammation with numerous abscesses (ABS) and cellulitis. Bones (B) and also necrosis of bone is visible (arrow). The abscess marked ABS* is shown with more detail in figure F. 2× magnification. (F) Detail of the abscess marked ABS* in the figure E. The arrows point at some of the bacterial colonies. The structure at the periphery of the

abscess (arrow-head) is shown in more detail in figure G.10× magnification. (G) Close view of the structure marked with an arrow-head in figure F. It exhibits necrotic leukocytes, bacteria and cell debris (***) surrounded by brightly eosinophilic, radial Splendore-Hoepli material (arrow-heads). Part of this material also appears intracellularly in degenerate and necrotic macrophages (arrows) positioned at the periphery of the abscess. The vast majority of cells visible in this figure are neutrophils. 60× magnification. (H) Detail of abscess in paw shows a colony of Gram-positive cocci immersed in exudate of neutrophils and also some macrophages. Gram stain. 60× magnification.

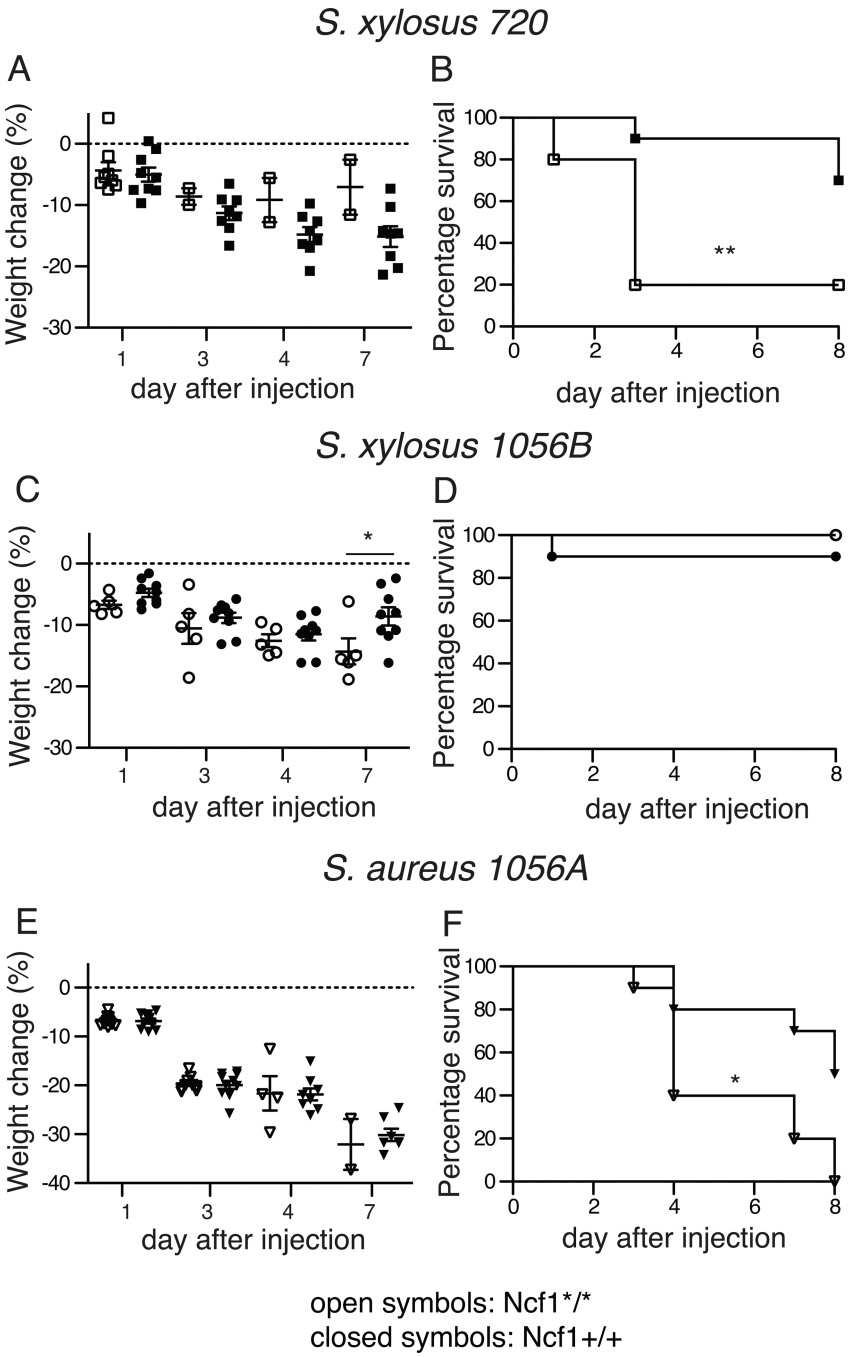

Figure 2. *Ncf1* mutant mice have increased susceptibility to systemic *Staphylococcus xylosus* and *Staphylococcus aureus* infections

0.8–1.4×10^8 bacteria of the two different strains of *S. xylosus* (720 and 1056 B) and the *S. aureus* 1056A isolated from infected paws of *Ncf1* mutant mice were injected i.v. into *Ncf1* mutant (Ncf1*/*) mice (N=10 for *S. aureus* and *S. xylosus* 720 and N=5 for *S. xylosus* 1056 A) and into wt (Ncf1+/+) mice (N=10). Mean and SEM is shown.

Weight loss (A, C and E) and survival (B, D, and F) were measured up to 7 days after bacterial challenge. Survival curves were displayed by Kaplan-Meier and intergroup comparisons assessed by the log-rank method. * P<0.05, ** P<0.01

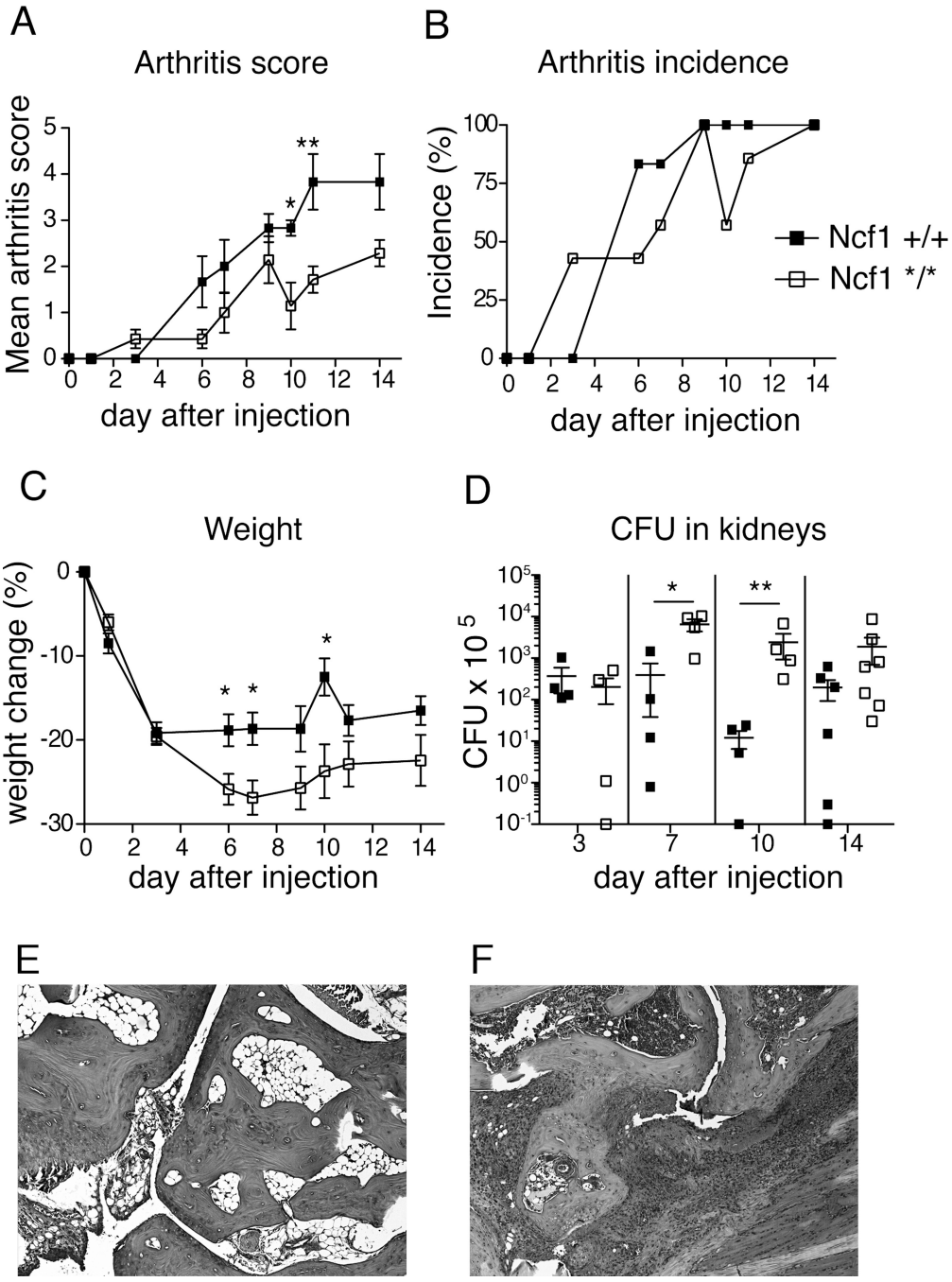

Figure 3. Weight loss and arthritis development after *S. aureus LS-1* i.v. injection in *Ncf1* mutant and wt mice

5.7×10^7 *S. aureus LS-1* was injected i.v. in *Ncf1* wt and mutant mice (n=19 mice per group). Arthritis severity and incidence (A and B) and weight (C) were evaluated over 14 days. (D) Four mice per group were sacrificed on day 3, 7, and 10, and the remaining 7 mice per group were sacrificed on day 14 after infection, and quantitative bacterial cultures were performed on kidneys. Mean and SEM is shown, except for incidence. * P<0.05, ** P<0.01. Statistics was calculated with Mann-Whitney for arthritis score and weight and with Kruskal-Wallis with Dunn's comparison post-test for bacterial cultures. On fig 3 A–C only the 7 mice/

genotype that were kept alive until day 14 are illustrated. (E–F) Histology of healthy and affected paw after injection of S. aureus LS-1, respectively. 5× magnification.

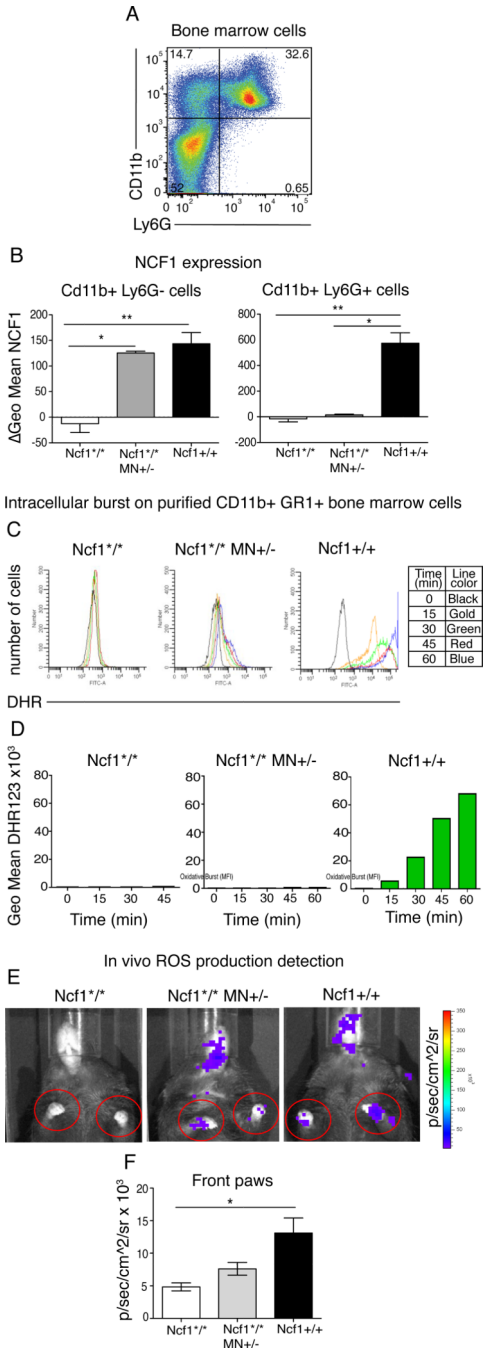

Figure 4. NCF1 expression and ROS quantification in bone marrow neutrophils from *Ncf1*/* MN +/− mice*

(A) Bone marrow cells were stained for surface markers CD11b (Mac-1, M1/70) and Ly6G (1A8) and gated accordingly. CD11b+ Ly6G− cells are considered as monocytes and CD11b+ Ly6G+ cells as neutrophils. (B) Intracellular NCF1 expression was measured in both cell populations. Mean and SEM of 5 animals per group is shown. (C) Intracellular ROS production was measured in purified on neutrophils from pooled bone marrows. After enrichment for neutrophils with Percoll gradient, cells were identified as neutrophils according to their scatter and CD11b and Ly6G expression by flow cytometry. DHR fluorescence was measured at different time points after PMA stimulation. Histograms with

different colors represent different time points: black 0 min, gold 15 min, green 30 min, red 45 min and blue 60 min. (D) Bar chart of the geo mean of DHR fluorescence at different time points after PMA stimulation. (E) *In vivo* oxidative burst imagining: luminescent probe L-012 was injected i.p. in naïve anesthetized mice and the luminescent signal was detected over 35 min by a CCD camera. Images illustrate a representative example for each genotype. (F) To quantify the *in vivo* oxidative burst, the luminescent signal was quantified at 15 min as photons/second/cm^2/steradian in the circled areas surrounding the front paws and the mean of the two front paws measurements was used. Mean and SEM of 5 mice per group. Statistical comparison is performed with Kruskal-Wallis with Dunn's comparison post-test.

Statistical significance between the groups indicated by a bar: * $P<0.05$, ** $P<0.01$, *** $P<0.001$.

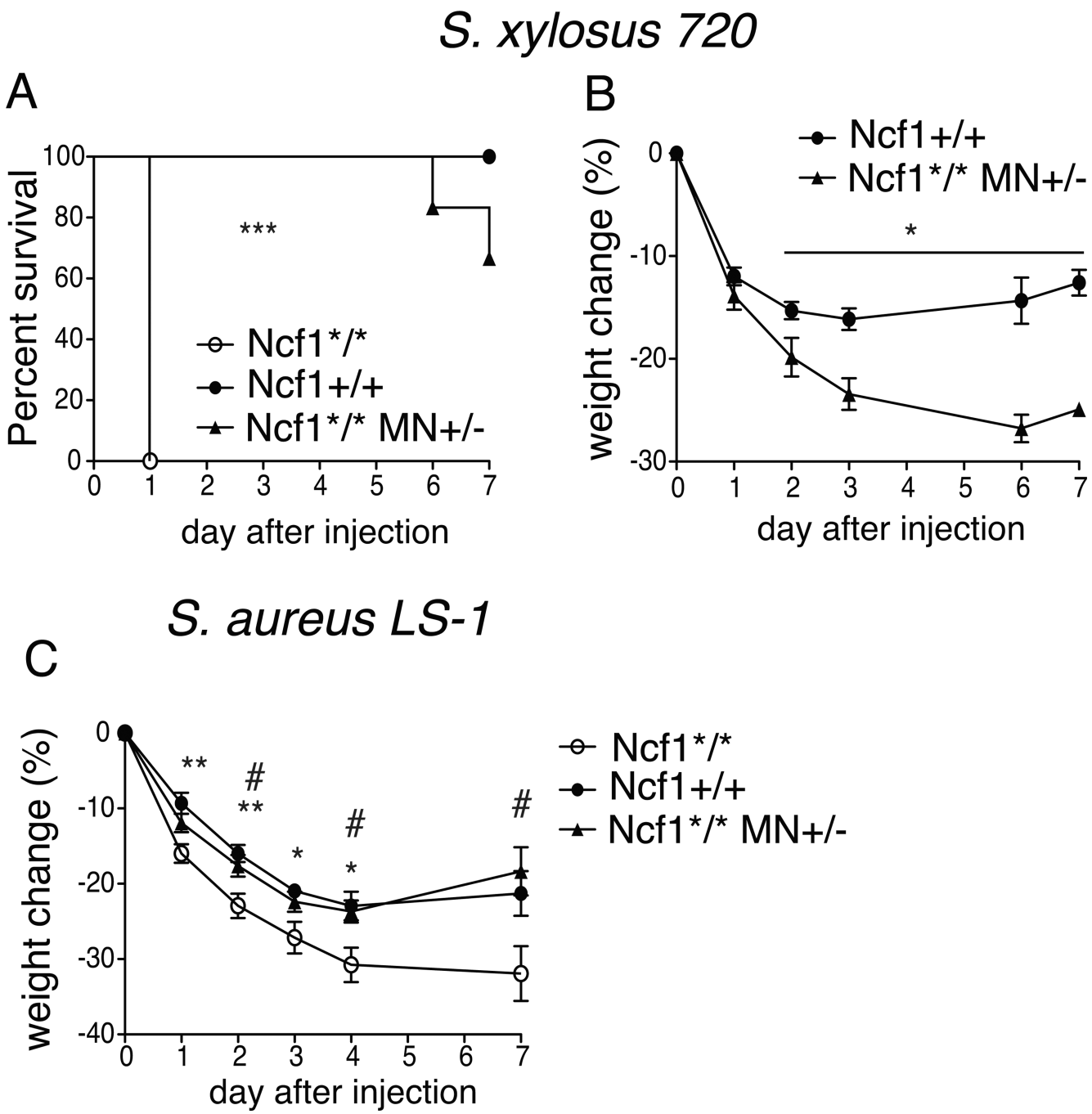

Figure 5. NCF1 expression in monocytes protects from *Staphylococci*

0.8×10^8 bacteria of *S. xylosus* 720 isolated from infected paws of *Ncf1* mutant mice were injected i.v. into *Ncf1*/* MN+/−* and non transgenic littermates *Ncf1*/** mice as well as *Ncf1 wt* (Ncf1+/+) mice (N=6–9). Survival (A) and weight change (B) were monitored over 7 days. Survival curves were displayed by Kaplan-Meier and intergroup comparisons assessed by the log-rank method: *** P<0.001. For weight changes, mean and SEM is shown and genotypes were compared using Mann-Whitney *P<0.05.

(C) Male *Ncf1*/* MN+/−* mice (N=9), as well as littermates negative for the transgene (*Ncf1*/**, N=10) and *Ncf1* wt (*Ncf1+/+*) (N=7) mice were injected i.v. with 5.7 × 10^7 *S. aureus* LS-1. Weight was monitored for 7 days. Mean and SEM is shown. * P<0.05 and **

P<0.01 between *Ncf1*/** and *Ncf1 +/+* mice, # P<0.05 between *Ncf1*/* MN+/−* and *Ncf1*/** calculated with Kruskal-Wallis with Dunn's comparison post-test.

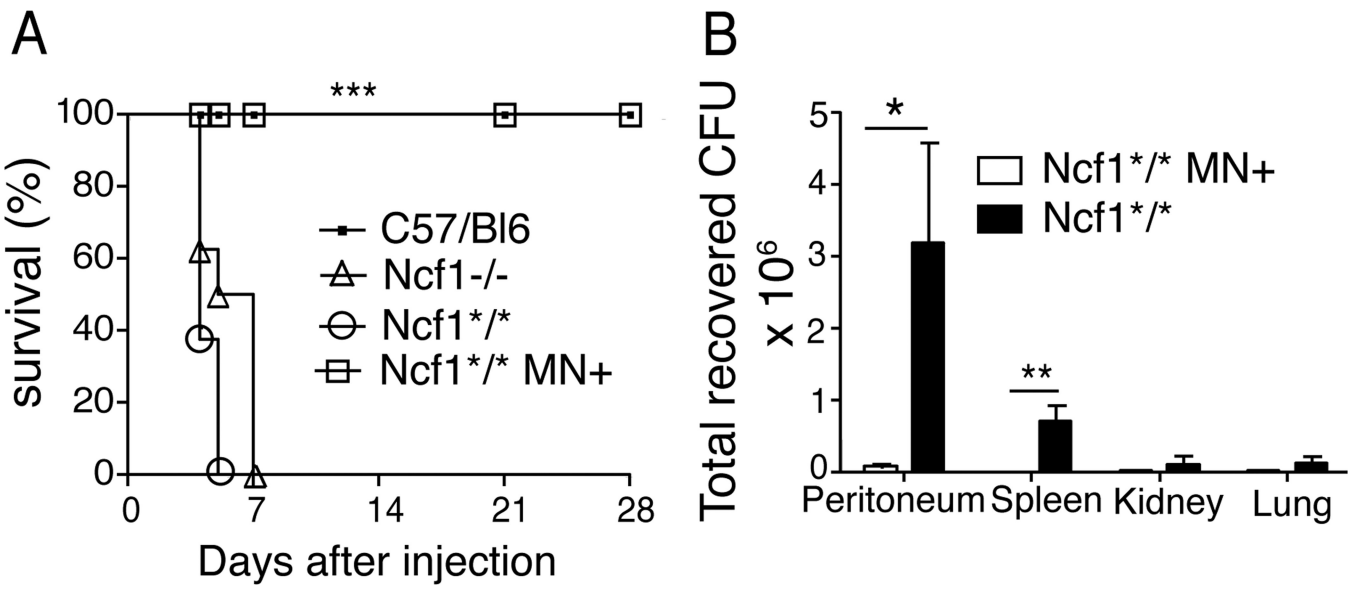

Figure 6. NCF1 expression in monocytes protects *Ncf1*/ mice from lethal *B. cepacia* infection**

B10.Q.Ncf1/* MN+* and *B10.Q.Ncf1*/** littermates negative for the transgene, *Ncf1−/−* and C57Bl/6 mice (N=10) were challenged i.p. with 4.5×10^5 *B. cepacia*. (A) Survival curves are displayed by Kaplan-Meier and intergroup comparisons between globally NADPH oxidase-deficient mice (*Ncf1*$^{-/-}$ and *Ncf1*/**) and *Ncf1*/* MN+* mice assessed by the log-rank method: *** P<0.001. (B) In separate studies, mice were administered i.p. 4×10^5 *B. cepacia* and bacteria load in peritoneal lavage, spleen, kidneys and lungs cell suspensions were quantified at 24h. Data are the combined results of two independent experiments; n= 8 mice per genotype. Mean and SEM is shown. * P< 0.004 using Mann Whitney test; ** p< 0.04 using Wilcoxon Signed Rank Test, which was used when bacterial cultures from a group were negative.

Table I

Number and frequency of observation of local infections in *Ncf1* mutant mice in the Stockholm mouse cohort[i]

Genotype	N° of observations			Total number of mice[b]	Frequency (%)
	Total	Males	Females[a]		
B10.Q.Ncf1*/*	27	21	6**	≈ 2000	≈ 1.3
B10.P.Ncf1*/*.MBQ	4	3	1	154	3
B10.Q.Ncf1*/*.uMT	13	9	4*	220	6
B10.Q.Ncf1*/*.COMPko	4	2	2	125	3
B10.Q.Ncf1*/*.TCRko	5	5	0	268	2
Total B10.Q.Ncf1*/* background	53	40	13***	≈ 2767	≈ 2

[a]Statistical significance for the gender difference was calculated with Chi-square test: * P<0.05, ** P<0.001, *** P<0.0001.

[b]The number of B10.Q.Ncf1*/* mice could only be estimated. For the other strains the total number of mice, males and females, is shown.

[i]Number of *Ncf1*/** mice from different lines with infections (most commonly in paws, nose, neck and ear) during 2009 and 2010. No infections were seen in any other mice, including the B10.Q.Ncf1+/+ (wt) controls or in heterozygous B10.Q.Ncf1*/+ mice. The frequency is calculated dividing the number of observed cases with the total number of *Ncf1*/* mice. B10.Q.Ncf1*/*.TCRko are lacking T cells (deficient in TCRb), B10.Q.Ncf1*/*.Bko are lacking B cells (deficient in the membrane part of IgM), B10.Q.Ncf1*/*.COMPko are deficient in COMP and B10.P.Ncf1*/*.MBQ express H2-A^q specifically on macrophages. They are all on the B10.Q.Ncf1*/* background and have been previously been described (15–17). Statistical significance for the gender difference was calculated with Chi-square test: * P<0.05, ** P<0.01, *** P<0.001.